Available online at www.sciencedirect.com
ScienceDirect
Ceramics International 36 (2010) 323–331
CERAMICS INTERNATIONAL
www.elsevier.com/locate/ceramint

Synthesis of SiC ceramics from processed cellulosic bio-precursor

Anwesha Maity [a], Dipul Kalita [b], Tarun Kumar Kayal [a], Tridip Goswami [b], Omprakash Chakrabarti [a,*], Himadri Sekhar Maiti [a], Paruchuri Gangadhar Rao [b]

[a] *Central Glass and Ceramic Research Institute, CSIR, Kolkata 700032, West Bengal, India*
[b] *North East Institute of Science and Technology, CSIR, Jorhat, Assam, India*

Received 2 January 2009; received in revised form 15 July 2009; accepted 12 August 2009
Available online 22 September 2009

Abstract

Synthesis of SiC ceramic from processed cellulosic bio-precursor was investigated. Bamboo (*Bambusa tulda* Roxb.) plants abundantly available in the Jorhat district of Assam, India, were selected for extraction of fibers following Kraft pulping method and bleached bamboo pulp fibers were suitably cast in the form of rectangular boards. Coir fibers available in the Alleppy district of Kerala, India, were initially digested with dilute alkali, mixed with cellulose acetate solution, air dried and then hot-pressed at 140 ± 5 °C under 2.0–2.5 MPa pressure to make rectangular boards. Well-characterized processed bio-precursors were pyrolysed at ∼800 °C under flowing N_2 atmosphere to prepare the bio-carbonaceous preforms (carbon templates) which showed nearly uniform shrinkages in all directions. Coir fiber composite board carbon showed lower pyrolytic weight loss (∼66%), higher density (0.49 g cm^{-3}), lower porosity (∼58%) and narrower pore diameter (10 μm) compared to the cast bamboo pulp fiber board carbon. The carbon samples showed perfect retention of fibrous morphological features of hierarchically grown bio-structures. Ceramization of carbon templates could be done by reactive melt silicon infiltration into porous channels at ∼1600 °C under vacuum. The final ceramics were adequately dense (%theoretical density > 99%), showed negligible linear dimensional changes (indicating net-dimension formation capability), presence of crystalline Si and SiC phases and duplex microstructure with complete preservation of fibrous architecture of plant bio-structure. The Si/SiC ceramic composite synthesized from coir fiber board gave room temperature 3-point flexural strength and Young's modulus values of 121 MPa and 276 GPa, respectively. Both the ceramic composites showed adequate oxidation resistance during heating at 1300 °C for 7 h in air.

Keywords: A. Processed bio-precursor; B. Fibrous morphology; C. Mechanical property; D. SiC ceramic

1. Introduction

Innovative synthesis of materials using biological world as a source has sparked considerable interest among the material scientist all over the globe [1,2]. A recent trend has been established in this direction to synthesize novel SiC-based ceramic materials from plant precursors (e.g. woods or stems [3–5], naturally grown fibers [6], hulls [7,8], etc.). Plants are light-weight, contain lignocellulosic matters, have fiber composite structures and exhibit adequate strength, rigidity, toughness, stiffness and damage tolerance. The cellular tissue anatomy of naturally grown plants is imitated into SiC ceramic structures with unique properties. In the bio-mimetic processing of SiC ceramics, plant precursor (e.g. woods or stems) is converted to skeletal bio-carbonaceous preform which on subsequent reaction with suitable Si bearing species, yields biomorphic or cellular SiC ceramics. Depending on the nature of processing, various morphologies (e.g. powder, fiber, monolith, composite, dense, porous, etc.) can be obtained. Since the microstructural development of the end ceramics is primarily guided by the initial cellular morphologies, characteristic features associated with the biological structures can have permanent imprint in the ceramic microstructures. Selectivity and anisotropy are two such features that can develop uniaxially oriented properties (anisotropic properties) [9], for example, flexural strength [10,11], porosity [12], electrical conductivity [13], etc. in cellular SiC ceramics, raising hopes of the new uses of the novel materials (filters, light-weight mechanically loaded structures, micro-heaters, etc.). It is equally important to mimic the fibrous biological

* Corresponding author. Tel.: +91 33 2473 3496; fax: +91 33 2473 0957.
E-mail address: omprakash@cgcri.res.in (O. Chakrabarti).

0272-8842/$36.00
doi:10.1016/j.ceramint.2009.09.006

architecture in cellular SiC ceramics with development of isotropic microstructure and property uniformity in all directions and dimensions. One possibility is to use processed bio-precursors in which the native fibrous morphological characteristics of biologically derived structures are preserved. Also, processed bio-precursors have the advantages of industrially manufactured products—the properties of processed bio-precursors (e.g. composition, density, porosity, pore size distribution, etc.) remain constant for different charges due to reproducible manufacturing process. Therefore, the aim of the present investigation is to examine the transformation of bio-organics with hierarchically built fibrous morphology present in the processed bio-precursor into SiC ceramic structures and to study the material, mechanical and thermo-chemical properties of the developed material.

2. Experimental

2.1. Preparation of processed cellulosic bio-precursor

Precursors to SiC ceramics were processed using two types of fibrous bio-structures—bamboo pulp fiber and coir fiber. Well matured bamboo (*Bambusa tulda* Roxb.) plants abundantly available in the Jorhat district of Assam, India, were harvested, cleaned, cut into chips of 10.0–12.5 mm size and oven dried. They were used for Kraft pulping and charged into a electrically heated rotary stainless steel digester (10 L capacity, Universal Engineering Corporation, Saharanpur, India). Required amount of chemical solution (17% active alkali ($NaOH:Na_2S$ = 3:1)) having a material to liquor ratio of 1:4 was added to the pulp charge. The cooking was done at 165 ± 2 °C for 3 h, keeping sulphidity fixed at 20%. Digested pulp was washed thoroughly with deionized water till free from alkali. Bleaching was carried out following hypochlorite alkali extraction–hypochlorite (H–E–H) sequence [14]. Bleached pulps were washed thoroughly with water and finally beaten in laboratory valley beater (Experimental Beater, S.O. A 7386, The Noble & Wood Machine Co., Hoosick Falls, NY, USA) at a consistency of 1.20%. After bleaching the fibrous morphology was completely retained (Fig. 1). The characteristics of

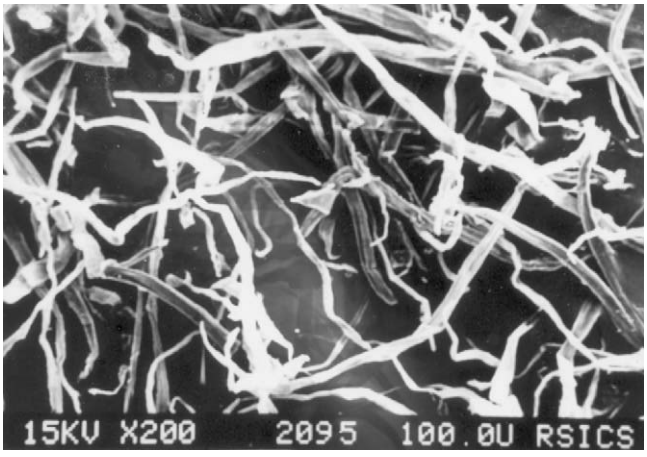

Fig. 1. SEM image of bleached bamboo pulp fibers.

Table 1
Molecular composition and other physico-chemical characteristics of plant fiber.

Characteristics of bio-structure specimen	Bamboo		Coir fiber
	Bamboo Species (*Bambusa tulda* Roxb.)	Bleached bamboo pulp fiber	
1. Chemical composition (%w/w)			
(a) Cellulose	57.40	78.12	36.44
(b) Lignin	25.90	0.08	39.84
(c) Pentosan	19.70	2.10	–
(d) Silica	4.30	0.08	0.02
(e) Pectic substance	–	–	3.00
(f) Ash content	1.70	0.35	2.10
2. Physical properties			
(a) Fiber properties	–		
(i) Max. length (mm)	–	2.80	1.01
(ii) Min. length (mm)	–	0.89	0.25
(iii) Av. length (mm)	–	1.45	0.98
(iv) Fiber diameter (μm)		17.00	222.00

bleached pulp fibers are presented in Table 1. The freeness of the pulp stock was initially measured to be 25°SR and was finally maintained at 45°SR. The pulp stock was sized with 3% solution of rosin and alum (Pragoti Chemicals, Jagi Road, Assam, India) and subsequently cast in the form of a rectangular board under vacuum. The cast pulp board was further pressed in a screw press (Gujrat Engineering Co., Gujrat, India) and finally dried in a hot press (Peeco Hydraulic Pvt. Ltd., Kolkata, India) at 75–85 °C. The characteristics of pressed boards are presented in Table 2.

Coir fibers were obtained from the Central Coir Research Institute, Alleppy, Kerala, India, cut to 1 cm size and digested with 6% NaOH (material to liquor ratio of 1:6) under boiling condition for 2 h in a stainless steel container. The digested fibers were thoroughly washed with deionized water till free from alkali, dried under sun, mixed with a solution of 20% cellulose acetate (Biolab, India) and partially dried in air for 2 h. The fibers were subsequently taken in a wooden mould and pressed in a hydraulic hot press at 140 ± 5 °C and 2–2.5 MPa pressure for 20 min. The pressed boards were found to be dense and have reasonably good mechanical properties (strength, elongation and breaking load) (Table 2).

2.2. Carbon template making

The bamboo pulp fiber and coir fiber boards were pyrolyzed at around 800 °C at a slow ramp under flowing N_2 atmosphere in a pyrolysis furnace (Stead Fast International, Kolkata, India) to make the carbon templates (C-templates). The C-templates, thus obtained, were tested for material properties (pyrolytic weight loss, dimensional shrinkages, bulk density and bulk porosity), crystallinity by X-ray diffraction (XRD) analysis (PW1710, Philips, Holland) using Cu Kα radiation of wave length λ = 1.5406 Å, pore size distribution by Hg-intrusion porosimetry (Poremaster, Quantachrome Instruments Inc., FL, USA) and microstructure by scanning electron microscopy (SEM) (SE-440, Leo-Cambridge, Cambridge, UK). The

Table 2
Characteristics of processed cellulosic bio-precursor.

Type of processed cellulosic bio-precursor	Mechanical properties			Weight loss upon drying at 100 °C for 24 h (%)	Bulk density (g cm^{-3})
	Tensile strength (MPa)	Elongation (%)	Breaking load (kg)		
1. Cast bamboo pulp fiber board	–	–	–	8.20	0.50
2. Coir fiber composite board	153	27.5	0.45	9.94	1.40

Raman spectra were recorded by a Spex double monochromator (Model 1403) equipped with a Spectra Physics Argon ion Laser (Model 2020-05) operated at 514.5 nm. The C-template sample was taken in a sample holder with the surface inclined at an angle of 45° to the laser beam and was excited at a power of 5 mW. Raman scattered radiation was collected at right angles to the excitation. The operation of photon counter, data acquisition and analysis were controlled by Spex Datamate 1B.

2.3. Ceramization of carbon template

Ceramization was done via melt Si infiltration processing technique. The C-templates were infiltrated and reacted with molten silicon at a temperature around 1600 °C for 1 h in a graphite resistance furnace (Astro, Thermal Technologies Inc., Santa Barbara, CA, USA) to yield SiC ceramics. The amount of Si infiltrant relative to the amount of carbon varied in the range of 0–3.5 Si:C mole ratio. The ceramics were characterized in terms of material properties–linear dimensional change, density (by water displacement method) and porosity (by boiling water method); crystallinity was examined by XRD analysis. Microstructural analysis was done by scanning electron microscopy. The room temperature flexural strength was determined in 3-point mode (span: 40 mm, cross-section: 4.75 by 3.25 mm^2, samples were ground and polished up to 1 μm finish and tensile surfaces were champhered) using an Instron Universal Testing machine. The deflection was monitored through a LVDT with a resolution of 0.05% of full scale deflection and from the load-deflection data, the Young's modulus was automatically obtained with the help of standard software. Five tests were conducted and an average value has been reported. The oxidation resistance was evaluated from the thermogravimetric analysis (STA 490 C, Netzcsh-Geratebau GmbH, Germany). Polished samples were taken in the form of small rectangular chip (∼6 mm × 5 mm × 0.4 mm, polished up to 1 μm diamond paste finish) and the tests were conducted up to 1300 °C in air with 7 h hold at the peak temperature. The weight gain recorded was converted to weight gain per unit area and plotted against time.

3. Results and discussions

3.1. Pyrolytic conversion of processed bio-precursor to carbon templates

3.1.1. Material properties

Both the precursor samples showed vast shrinkages in major dimensions (length, width, thickness) during pyrolysis. The C-templates were found to have reasonably good structural integrity without any sign of cracks and delamination. The pyrolytic shrinkage and weight loss data are presented in Table 3. Both the samples showed nearly uniform pyrolytic shrinkages in all directions. This was different from the pyrolytic shrinkage characteristics of naturally grown plant precursors (e.g. woods or stems), which exhibit anisotropic pyrolytic shrinkages [15]. The isotropic shrinkages might arise from uniform distribution of fibrous bio-structures in the processed precursors and would probably be helpful to achieve directional property homogeneity for the ceramic materials synthesized from such precursors.

Pyrolyzed bamboo pulp fiber boards exhibited lower density and higher porosity than the coir fiber board carbon samples. The bamboo pulp fiber contained high weight percentage of cellulose with negligible content of lignin; coir fiber contained 36.4 and 39.8% of cellulose and lignin, respectively. The losses in weight during pyrolysis at temperatures >400 °C, for cellulose and lignin are ∼85% [16] and 65% [17], respectively. Higher loss of weight during pyrolysis of bamboo pulp fiber board samples was, therefore, reasonable and resulted in higher porosity and lower density. The lower pyrolytic weight loss likely resulted in higher bulk density and lower porosity for the coir board C-template samples.

3.1.2. XRD analysis

Fig. 2 shows the XRD profiles of C-templates obtained from the two types of processed precursors. There were two main graphitic peaks corresponding to a broad ($2\theta = 26.6$) peak and a low intensity ($2\theta = 44.6$) peak. The results indicated that the C-template samples were amorphous.

Table 3
Characteristics of carbon template.

Types of C-template	Pyrolytic weight loss (%)	Dimensional shrinkage (%)			Volume shrinkage (%)	Density (g cm^{-3})	Bulk porosity (%)
		Length	Width	Thickness			
1. Cast bamboo pulp fiber board	72.76	21.77	21.69	21.76	52.07	0.2449	70.37
2. Coir fiber composite board	66.66	19.10	19.09	17.31	46.02	0.4964	58.37

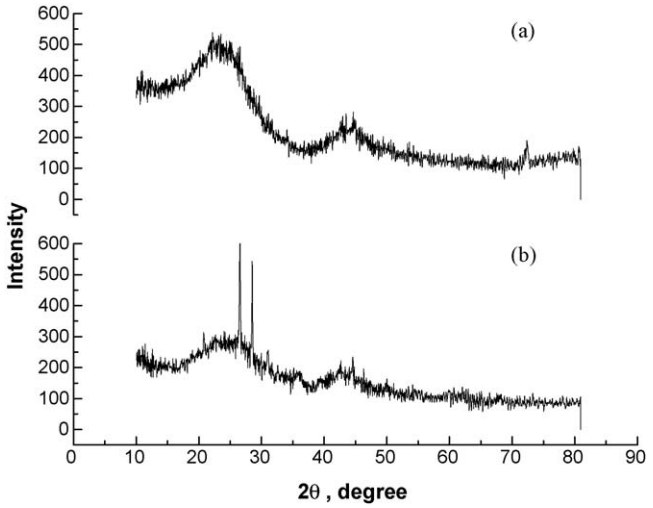

Fig. 2. XRD profile of carbon template obtained from (a) coir fiber board and (b) bamboo pulp fiber board.

3.1.3. Pore size distribution

Pore size distribution patterns of the C-templates obtained from two types of precursors are shown in Fig. 3. Bamboo pulp fiber board carbon showed multimodal pore size distribution with broad peaks at 40–60, 10–20, 5–8 and 2–3 μm and relatively sharp peaks at 8–9 and 4–5 μm pore diameters. The results indicated that pores with diameter in the range of 10–25 μm made maximum contribution (around 56%) to the total porosity. Coir fiber board carbon also showed multimodal pore size distribution with four sharp peaks at 8–9, 6–7, 0.4–0.5 and 0.2–0.3 μm and six broad peaks at 40–100, 30–40, 25–30, 18–25, 9–18 and 4–6 μm pore diameters. Two major contributions to the total porosity were noticed—nearly 33% and 34% from pores of with diameter in the range of 0.01–0.6 and 30–100 μm, respectively. The total porosity and the average pore diameters for pyrolyzed bamboo pulp fiber and coir fiber boards were found to be 70.37% and 14.17 μm and 58.37% and 10.65 μm, respectively.

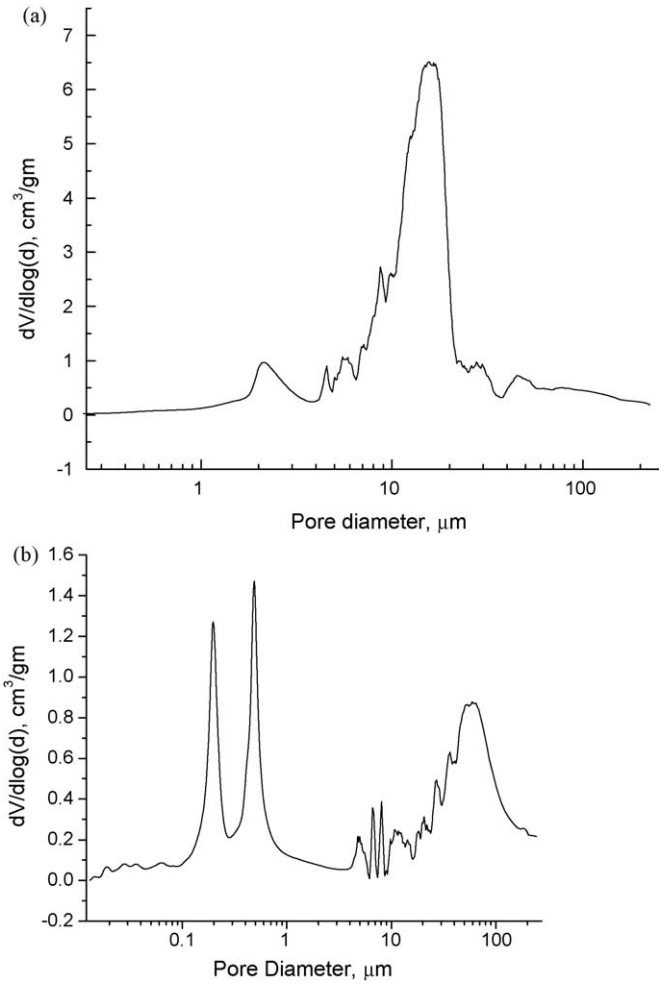

Fig. 3. Pore size distribution pattern of carbon template obtained from (a) bamboo pulp fiber board and (b) coir fiber board.

3.1.4. Microstructural analysis

Microscopic examination of C-templates made from bamboo pulp fiber board showed porous fibrous microstructure. The morphology of native cellulose fibers was seen to be well preserved (Fig. 4(a)). Pores were seen to have formed by networking of the carbon fibers consisting of crossover,

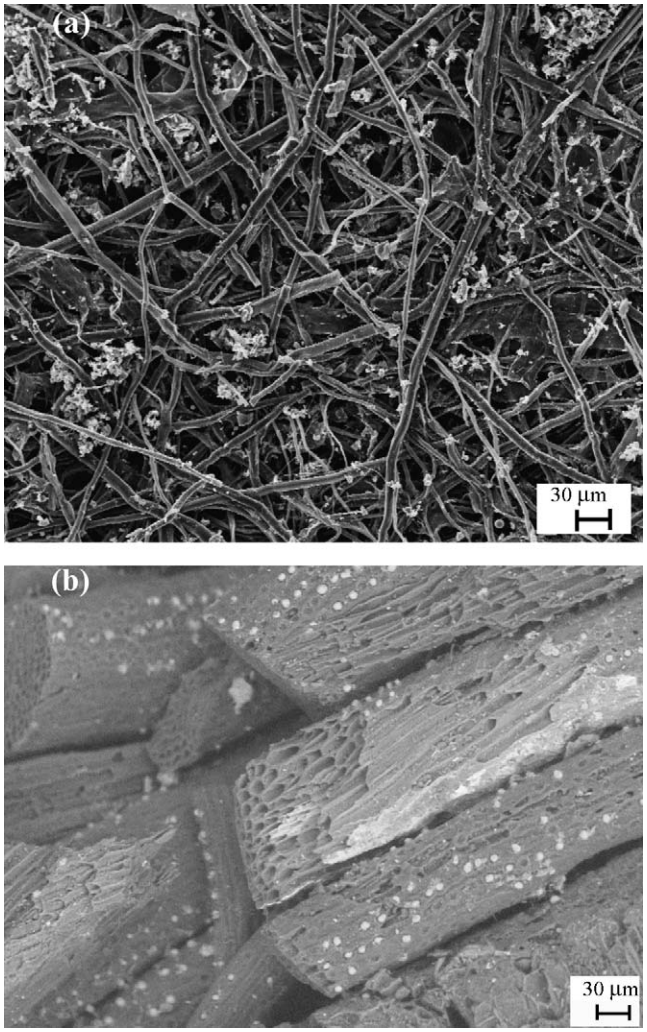

Fig. 4. SEM image of carbon template obtained from (a) coir fiber board and (b) bamboo pulp fiber board.

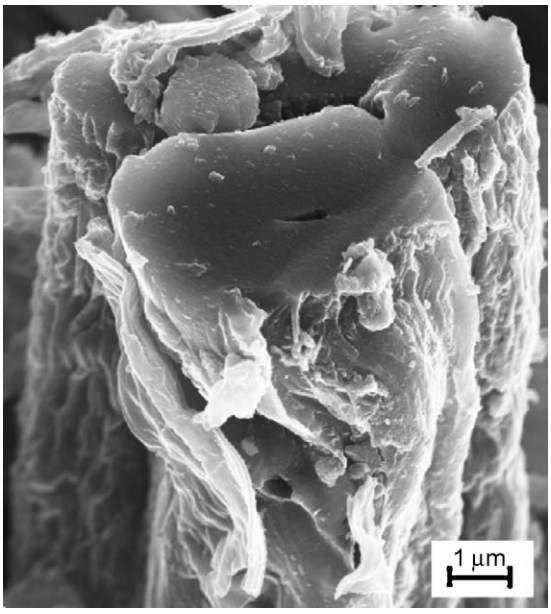

Fig. 5. Higher magnification FESEM image of carbon template obtained from bamboo pulp fiber board showing nearly solid structure of carbon fiber.

underpass and even branching of a single filament. Dimensional uniformity in a single filament was seen to be maintained. Diameter of carbon filaments varied in the range of 4–14 μm. Higher magnification field effect SEM imaging (Fig. 5) revealed that the individual filaments were solid. Also the pore diameters were found to be consistent with the results obtained in the Hg-intrusion porosimetry test. Microstructure of coir fiber board carbon showed fibrous morphology of coir carbon embedded in a carbonaceous matrix derived from cellulose acetate derivative and pores were mostly formed by networking of the carbon filaments (Fig. 4(b)). Diameters of carbon filaments were seen to vary in the range of around 20 to more than 100 μm. They were porous and each of them consisted of cellular channels of diameters varying from sub-micron to few micrometer sizes. Microscopic measurements of pore diameters were in close agreement with the porosimetry results.

3.1.5. Raman spectroscopy

Fig. 6 shows the Raman spectra of C-templates obtained from the two types of processed precursors. Raman bands appeared at the positions of approximately 1350 and 1600 cm^{-1}. These bands are assigned to in-plane vibrations of sp^2-bonded carbon with structural imperfections (D band) and in-plane vibrations of sp^2-bonded carbon without structural imperfections (crystalline carbon (G band)), respectively and are reported in the literature [18,19]. The Raman spectra of carbonized specimens from the two processed precursors showed no appreciable difference.

3.2. Ceramization via melt silicon infiltration processing

Ceramization was done at a temperature of 1600 °C for a period of 1 h following reactive melt silicon infiltration processing technique. Infiltration occurred spontaneously when

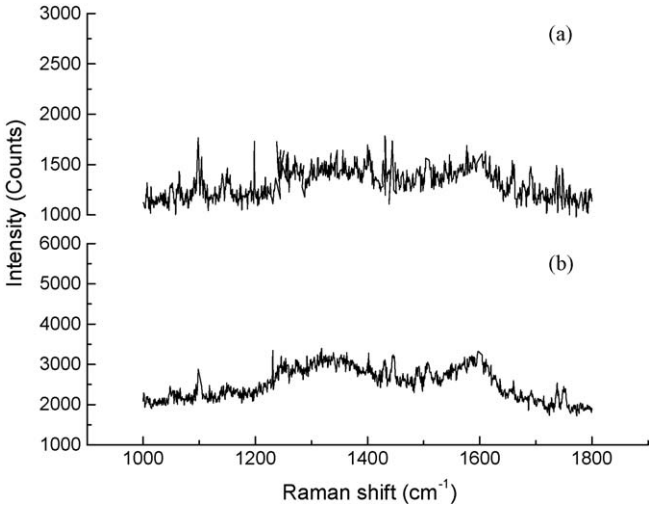

Fig. 6. Raman spectra of C-templates made from (a) bamboo pulp fiber board and (b) coir fiber board.

the carbon templates were suitably brought in contact with the infiltrating melt (liquid Si). The amount of infiltrant (e.g. Si) relative to the weight of the carbon template varied in the range of 0–3.5 Si:C mole ratio, i.e., from under-stoichiometric to over-stoichiometric amount of silicon needed for conversion of C to SiC. Depending on the amount of Si infiltrant added processing of the porous and dense SiC-based ceramics could be possible. Si has a vapour pressure of 6.3×10^{-5} atm. at the infiltration processing temperature [20]; excess addition of infiltrant might be justified to yield a SiC material. Usage of large excess of infiltrant could produce dense Si/SiC duplex composite. Infiltrating Si was expected to convert the carbon pore wall to SiC and the residual Si was likely to fill in the remaining pore interior. Si in the pore solidified on cooling.

3.2.1. Material property of infiltrated specimen

Reactive infiltration consists of two processes occurring simultaneously: (a) infiltration and (b) reaction. In the present investigation capillary infiltration of liquid Si into porous carbon preforms could be explained by the simple Washburn model [21]. The model assumed the pore medium as a constant capillary and can be represented as

$$h^2 = r\gamma \cos\frac{\theta t}{2\eta} \quad (1)$$

where h is the infiltrated distance, t is the time, η is the fluid viscosity, γ is the surface tension, r is the pore radius and θ is the wetting angle. Using reported property data of liquid Si at 1600 °C ($\eta = 0.7$ mPa [22], $\gamma = 0.82$ Nm^{-1} [22] and $\theta = 10°$ [23]), infiltration depth (h) could be estimated as a function of time (t) for carbon specimens made from both the precursors (Fig. 7). Infiltration depth was estimated to be in the range of 3.4–3.8 m for $t = 1$ h. It indicated that liquid Si might readily be infiltrated in to carbonized processed precursors used in the present study. For the C–Si reaction, the mechanistic model proposed by Fitzer and Gadow [24] could be used. It stated that the combined reaction process includes mass transport from

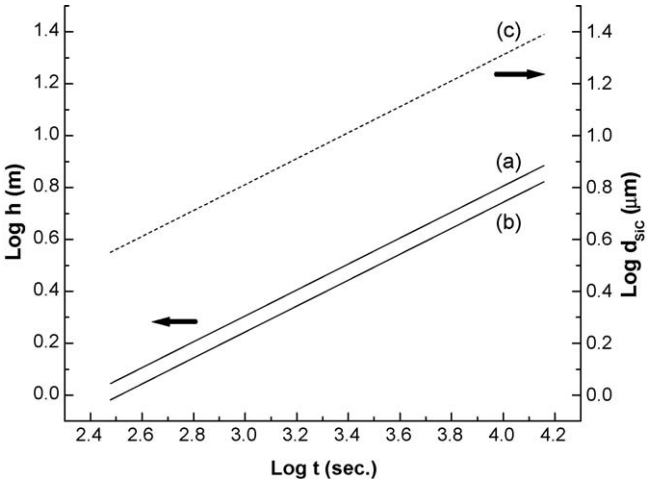

Fig. 7. Melt Si infiltration height vs. infiltration time for carbonized processed precursor of (a) bamboo pulp fiber board and (b) coir fiber composite board; (c) growth of SiC reaction layer as a function of time is shown by dashed line.

liquid Si to solid carbon, diffusion of atomic Si through SiC layer (d_{SiC}) and reaction between Si and carbon—the diffusive movement of Si is the rate determining step. Following expression for the growth kinetics can be derived from the model:

$$d_{SiC} = \sqrt{(D_{eff}t)} \quad (2)$$

where D_{eff} is the effective diffusion coefficient and t is the time. From the values of D_{eff} (4.2×10^{-10} cm^2 s^{-1}) [24], the thickness of reaction-formed SiC layer was derived as a function of time and presented in Fig. 7; SiC layer thickness could be estimated to be around 12 μm for t = 1 h. In the present case, the infiltration time might be sufficient for conversion of bamboo carbon filaments of average diameter of 9 μm. Though the coir carbon fiber had an average diameter of 60 μm, the filaments appeared to be porous with channel wall thickness of 2–5 μm only; hence an hour might be sufficient for conversion of coir carbon fiber to SiC.

Assuming (i) no loss of carbon during ceramization and (ii) no volumetric change before and after ceramization, material properties of the ceramic could be predicted by the following set of empirical equations (also see Appendix):

$$\rho_{ceram} = \rho_c + x \quad (3)$$

$$P_{ceram} = \{1 - (0.500\rho_c + 0.231x)\}100 \quad (4a)$$

$$P*_{ceram} = \{1 - (0.038\rho_c + 0.429x)\}100 \quad (4b)$$

where ρ_{ceram} is the ceramic density, P_{ceram} and $P*_{ceram}$ are the ceramic porosity for under-stoichiometric and over-stoichiometric addition of infiltrant silicon, respectively, x is the amount of infiltrant silicon and ρ_c is the bulk density of the C-template. The material properties of the ceramics were measured and compared with the predicted values (Fig. 8). The density and porosity of the ceramics made from both the processed bio-precursors were found to be nearly tallying with the theoretically predicted data. At any Si:C mole ratio SiC ceramic synthesized from coir fiber composite board exhibited higher density and lower porosity than its counterpart made from the

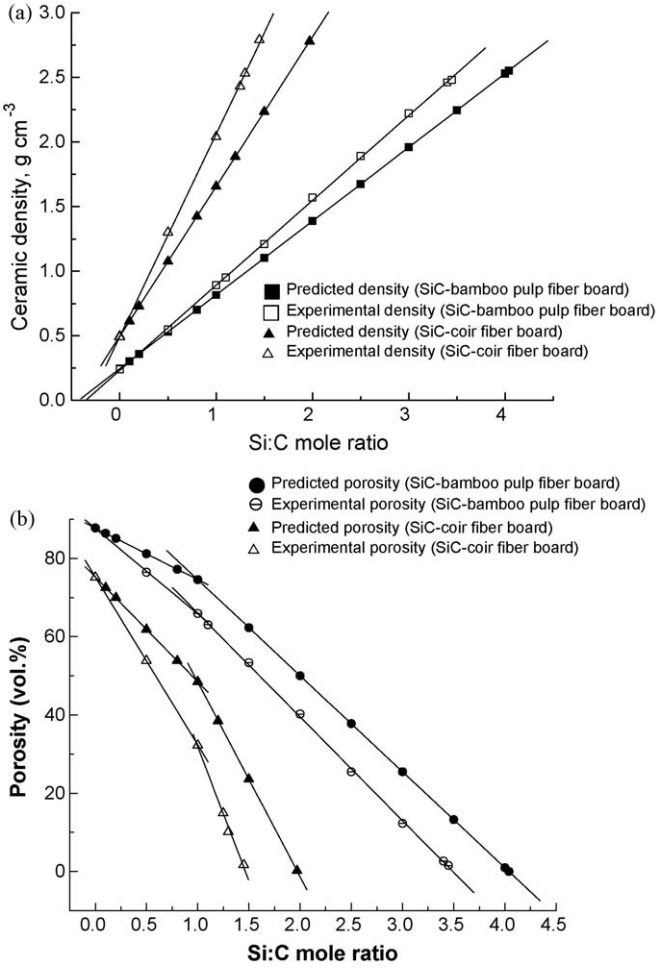

Fig. 8. Plots showing predicted and practical interdependence between (a) Si:C mole ratio and ceramic density and (b) Si:C mole ratio and ceramic porosity.

bamboo pulp fiber board precursor. Also, in comparison to theoretically predicted values, slightly higher density and lower porosity were obtained. During infiltration run, 800 °C carbon templates were likely to have undergone rearrangement resulting in increase of crystallinity and degree of order of graphite-like structural units [3]. This effect was significant at the infiltration temperature of 1600 °C, causing increase of density of starting carbon preform [12]. This might have resulted in lower experimental porosity and higher experimental density. After ceramization, the linear dimensional changes were measured and found to less than 1% in majority of the cases, indicating net shape formation capability.

3.2.2. XRD analysis

XRD analysis of final ceramic products indicated that the material was a kind of duplex composite consisting of β-SiC and Si phases. The XRD profiles of ceramics made from bamboo pulp and coir fiber board precursors are shown in Fig. 9. When the porous channels of the C-templates were subjected to incoming Si from all directions, Si completely occupied the channels with the conversion of carbonaceous pore wall to SiC and pore interior was filled in with residual Si. In case of availability of enough amount of Si, pore interior

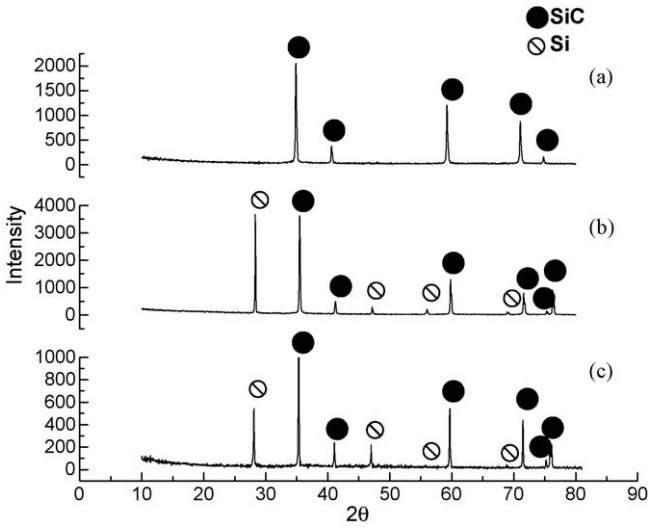

Fig. 9. XRD profile of Si-infiltrated pyrolyzed processed bio-precursor samples showing (a) absence and (b and c) presence of residual Si phase depending on processing conditions—(a) SiC ceramic and (b) Si/SiC composite from bamboo pulp fiber board and (c) Si/SiC composite from coir fiber board.

could be completely filled in with remaining Si, resulting in formation of dense Si/SiC composite products. With the decreasing amount of infiltrant Si, the intensity of residual Si phase decreased or even disappeared.

3.2.3. Microstructure

Fig. 10 shows the microstructure of dense Si/SiC composites made from two types of processed precursors. For both the materials sections cut along the major dimensions were viewed under microscope and hardly any difference could be noticed, indicating isotropic nature of the microstructure. During SEM examination of the dense Si-infiltrated pyrolyzed coir fiber board sample, three phases were observed (i) dark grey regions, (ii) light grey regions and (iii) occasional deep black spot (region (i) and (ii) mostly appear together) (Fig. 10(a)). Phases (i) and (ii) were identified as SiC and Si, respectively by EDX analysis and deep black spots were identified as pores and/or residual carbon. Similar phases were also noticed in the microstructure of dense Si-infiltrated pyrolyzed bamboo pulp fiber board sample (Fig. 10(b)). Some occasional presence of white spots was also noticed in the microstructure of Si/SiC ceramic made from bamboo pulp fiber board. Their formation might be related to the trace elements present in the native plant. Plants possess different trace elements (Fe, Mn, Al, Ca, K, Mg, Na). Of these elements iron and aluminum in particular are often present in monocotyledonous plants like bamboo, paddy, coconut, etc. [8,25]. During melt Si infiltration run complex silicide comprising of Si, Al and Fe might have formed resulting in formation of white spots. Occasional presence of such complex ternary silicide was also observed in the microstructure of alloyed Si/Mo melt infiltrated carbonaceous performs [26].

3.2.4. Mechanical property

The dense Si/SiC ceramic composite (having a density and porosity of 2.69 gm cm^{-3} and 1.9 volume%, respectively) made from coir fiber board precursor was tested for flexural strength and Young's modulus. The room temperature strength and elastic modulus was found to be 120 ± 14 MPa and 276 ± 35 GPa, respectively. Si/SiC ceramics synthesized from different types of woods (e.g. monocotyledonous coconut, dicotyledonous mango, jackfruit and teak and gymnosperm pine) exhibits variation of density and porosity in the ranges of 2.52–2.79 gm cm^{-3} and 0.8–1.2 volume%, respectively [27]; their room temperature strength and elastic modulus values also vary in the ranges of 180–247 MPa and 193–253 GPa, respectively [27]. Compared to the ceramics made from natural precursors (woods), ceramics synthesized from processed precursors exhibited lower strength; their elastic moduli were nearly comparable. The low value of strength of the ceramics synthesized from coir fiber board might be related to the coarse fibrous structure of the material.

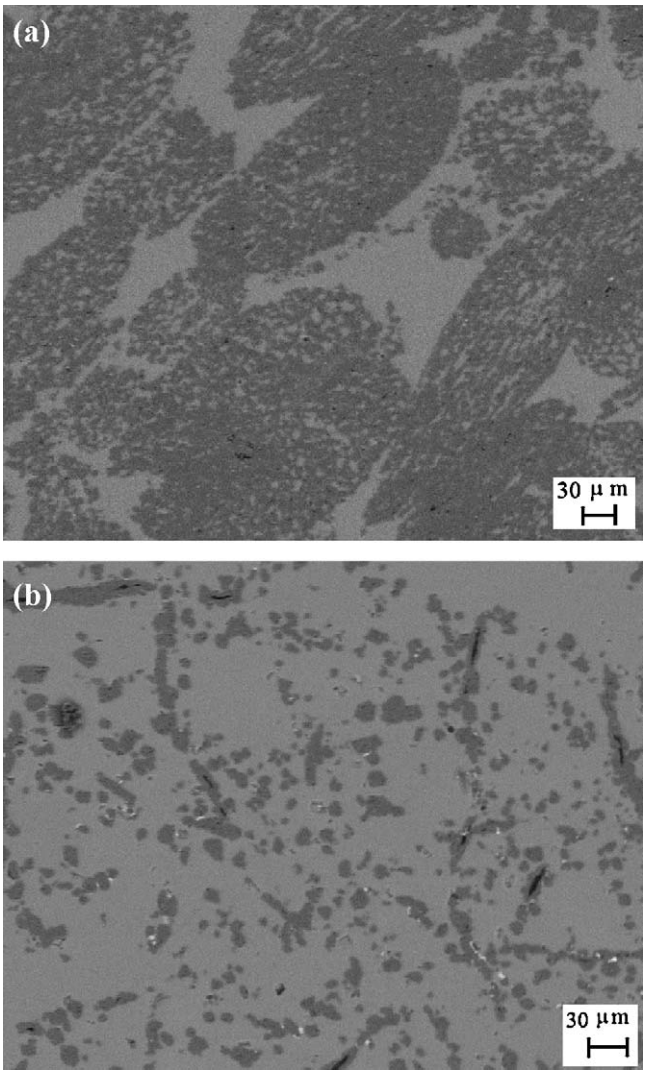

Fig. 10. Representative SEM images of dense Si/SiC ceramic composites synthesized from (a) coir fiber board and (b) bamboo pulp fiber board precursor.

3.2.5. Oxidation resistance

Thermal analysis (thermogravimetry) results of the dense Si/SiC ceramics synthesized from processed precursors exhibited

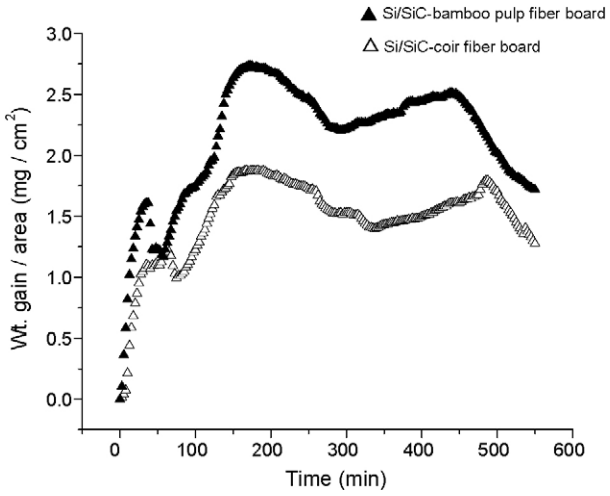

Fig. 11. Oxidation resistance of dense Si/SiC ceramic composite synthesized from processed bio-precursors at 1300 °C in air.

a small increase in weight per unit area during heating up to 1300 °C in flowing air, indicating appreciable oxidation resistance of the final ceramic (Fig. 11). XRD analysis of the post-oxidation sample indicated that the increase in weight was due to the formation of protective SiO_2 surface layer as a product of oxidation. This SiO_2 was expected to have prevented further ingress of oxygen to react with SiC and Si [28]. Si/SiC composite derived from coir fiber board showed higher resistance to oxidation up to 1300 °C, compared to ceramic made from bamboo pulp fiber board, probably because of higher density.

4. Conclusion

The present study could demonstrate the possibility of producing novel SiC ceramics using processed bio-precursors. The bio-precursors could be processed following casting of bamboo pulp fibers and compositing coir fibers with cellulose acetate. Ceramics could be produced following a two-step processing—conversion of bio-precursors to C-templates via pyrolysis and ceramization of C-templates via reactive melt Si infiltration technique. Both the C-templates and the end ceramics could retain the fibrous morphological features present in processed bio-precursors. Depending on the amount of Si infiltrant added, formation of porous and dense morphologies of SiC ceramics could be controlled. The biomorphic duplex Si/SiC ceramic composites were extremely dense (with %T.D. > 99%), exhibited net shape formation capability and showed reasonably good mechanical properties. Si/SiC ceramic composites synthesized from coir fiber composite board precursor typically exhibited room temperature flexural strength and Young's modulus of 120 MPa and 276 GPa, respectively. The dense duplex composites derived from the two types of processed bio-precursors showed high oxidation resistance during heating at 1300 °C in flowing air. The novel ceramic composites have tremendous application potentials as light-weight mechanically loaded structures at high temperature hostile atmospheres, kiln furniture, mechanical pump seals, armour ceramics, etc.

Acknowledgements

The authors wish to thank Dr. D.K. Bhattacharya, Head, Analytical Facility Division, CGCRI and Mr. P. Sengupta, Head, Materials Science Division, NEIST, for active support for undertaking the collaborative work. They also wish to thank the staff-members of Non-Oxide Ceramic and Composite Division, CGCRI and Cellulose, Paper and Pulp Division, NEIST, for their cooperation and help. They further express their thanks to Prof. M. Ghosh, Prof. G.B. Talapatra and Prof. T. Ganguly of Department of Spectroscopy, Indian Association for Cultivation of Science (IACS), Kolkata, India, for their support and cooperation to carry out Raman Spectroscopic studies at IACS. Finally they are thankful to the Director, CGCRI, and Director, NEIST, for according permission to publish this work.

Appendix A. Interrelations of materials parameters for reactive infiltration

Let x be the weight of Si per unit volume of carbon preform, consumed for ceramization of carbon preform via reactive infiltration. Then the total weight of ceramic per unit volume is given as $\rho_c + x$, which yields Eq. (3). In Eq. (3) ρ_c represents the bulk density of carbon in units of g cm^{-3}.

A.1. Porosity of ceramic synthesized by consumption of over-stoichiometric amount of Si

The expression for obtaining the amount of SiC formed is $(40\rho_c/12)$gm, where the values 40 and 12 represent the respective molecular weights of SiC and carbon. Given the density of SiC (3.21 g cm^{-3}), the volume of SiC is given as the quantity $[40\rho_c/(12 \times 3.21)]$cc.

The expression for obtaining the amount of Si consumed for stoichiometric conversion to SiC is $(28\rho_c/12)$gm, where the value 28 represents the molecular weight of Si; or the remaining infiltrant is given by the quantity $[x - (28\rho_c/12)]$gm. Given the density of Si (2.33 g cm^{-3}), the volume of remaining infiltrant is given by the quantity $[\{x - (28\rho_c/12)\}/2.33]$cc.

Assuming that no dimensional change during reactive melt infiltration process and assuming that the remaining infiltrant occupies the excess porosity, the expression for obtaining the fractional volume of porosity is

Fractional pore volume $= 1 - [40\rho_c/(12 \times 3.21) + \{x - (28\rho_c/12)\}/2.33]$, which yields Eq. (4(b)).

A.2. Porosity of ceramic synthesized by consumption of under-stoichiometric amount of Si

The expression for obtaining the amount of SiC formed is $(40x/12)$gm and the volume of SiC is given as the quantity $[40x/(12 \times 3.21)]$cc.

The expression for obtaining the amount of carbon consumed for conversion to SiC is $(12x/28)$gm; or the remaining carbon is

given by the quantity $[\rho_c - (12x/28)]$gm. Given the density of C (2.00 g cm^{-3}) [12], the volume of remaining carbon is given as the quantity $[\{\rho_c - (12x/28))\}/2.00]$cc.

Then the expression for obtaining the fractional volume of porosity is

Fractional pore volume = $1 - [40x/(12 \times 3.21) + \{\rho_c - (12x/28))\}/2.00]$, which yields Eq. (4(a)).

References

[1] A.V. Srinivasan, G.K. Haritos, F.L. Hedberg, Biomimetics: advancing man-made materials through guidance of nature, Appl. Mech. Rev. 44 (11) (1991) 463–482.

[2] A.H. Heuer, D.J. Fink, V.J. Laraia, J.L. Arias, P.D. Calvert, K. Kendell, G.L. Messing, J. Blackwill, P.C. Rieke, D.H. Thomson, A.P. Wheeler, A. Veis, A.I. Caplan, Innovative materials processing strategies: a biomimetic approach, Science 255 (1992) 1098.

[3] P. Greil, T. Lifka, A. Kaindl, Biomorphic cellular silicon carbide ceramics from wood: I. Processing and microstructure, J. Eur. Ceram. Soc. 18 (14) (1998) 1961–1973.

[4] M. Singh, Environment conscious ceramics, Ceram. Eng. Sci. Proc. 21 (4) (2000) 39–44.

[5] O.P. Chakrabarti, H.S. Maiti, R. Majumdar, Si/SiC ceramics from plant precursor, J. Mater. Sci. 39 (14) (2004) 4715–4717.

[6] R.V. Krikrishnarao, Y.R. Mahajan, Preparation of silicon carbide fiber from cotton fiber and silicon nitride, J. Mater. Sci. Lett. 15 (1–6) (1996) 1232–1235.

[7] J.E. Lee, I.B. Cutler, Formation of silicon carbide from rice hulls, Am. Ceram. Soc. Bull. 54 (1975) 195–198.

[8] A. Selvam, N.G. Nair, P. Singh, Synthesis and characterization of SiC whiskers from coconut shell, J. Mater. Sci. Lett. 17 (1) (1998) 57–60.

[9] P. Greil, Biomorphous ceramics from lignocellulosics, J. Eur. Ceram. Soc. 21 (2001) 105–118.

[10] P. Greil, T. Lifka, A. Kaindl, Biomorphic cellular silicon carbide ceramics from wood: II. Mechanical properties, J. Eur. Ceram. Soc. 18 (14) (1998) 1974–1983.

[11] J. Martinez-Fernandez, F.M. Valera-Feria, M. Singh, High temperature compressive mechanical behaviour of biomorphic silicon carbide ceramics, Scripta Mater. 43 (2000) 813–818.

[12] A. Harzog, R. Klingner, U. Vogt, T. Graule, Wood derived porous ceramics by sol infiltration and carbothermal reduction, J. Am. Ceramic. Soc. 87 (5) (2004) 784–793.

[13] D. Mallick, O.P. Chakrabarti, D. Bhattacharya, M. Mukherjee, H.S. Maiti, R. Majumdar, Electrical conductivity of cellular Si/SiC ceramic composites prepared from plant precursors, J. Appl. Phys. 101 (033707) (2007) 1–7.

[14] T. Goswami, C.N. Saikia, R.K. Baruah, C.M. Sarma, Characterization of pulp obtained from *Populus Deltoides* plants of different ages using IR, XRD and SEM, Biores. Technol. 57 (1997) 209–214.

[15] D. Mallick, O.P. Chakrabarti, H.S. Maiti, R. Majumdar, Si/SiC ceramics from wood of Indian dicotyledonous mango tree, Ceram. Intl. 33 (2007) 1217–1222.

[16] D.N.S. Hon, Wood and Cellulose Chemistry, Marcel Dekker Inc., New York, 1991.

[17] J. Schmork, The Chemistry of Cellulose and Wood, Oldbourne Press, 1966.

[18] F. Tuinstra, J.L. Koenig, Raman spectrum of graphite, J. Chem. Phys. 53 (3) (1970) 1126–1130.

[19] M. Nakamizo, H. Honda, M. Inagaki, Raman spectra of ground natural graphite, Carbon 16 (4) (1978) 281–283.

[20] C.L. Yawas, X. Lin, L. Bu, D.R. Balundgi, S. Tripathi, Vapor pressure, in: C.L. Yaws (Ed.), Chemical Properties Hand Book, Mc-Graw Hill, New York, 1999, pp. 182–183.

[21] E.W. Washburn, The dynamics of capillary flow, Am. Phys. Soc.: 2nd Ser. (1921) 374–375.

[22] W. Krenkel, F. Gern, Microstructure and characteristics of CMC manufactured via liquid phase route, in: Proceedings of the 9th International Conference on Composite Materials, ICCM-9, Madrid, Spain, July, (1993), pp. 12–16.

[23] T.J. Whalen, A.T. Anderson, Wetting of SiC, Si_3N_4 and carbon by Si and binary Si alloys, J. Am. Ceram. Soc. 58 (9–10) (1975) 396–399.

[24] E. Fitzer, R. Gadow, Fiber reinforced silicon carbide, Am. Ceram. Soc. Bull. 65 (2) (1986) 326–335.

[25] M. Patel, A. Karera, SiC whiskers from rice husk: role of catalysts, J. Mater. Sci. Lett. 8 (1989) 955–956.

[26] O.P. Chakrabarti, P.K. Das, Reactive infiltration of Si–Mo alloyed melt into carbonaceous preforms of silicon carbide, J. Am. Ceram. Soc. 83 (6) (2000) 1548–1550.

[27] O.P. Chakrabarti, H.S. Maiti, R. Majumdar, Final Technical Report of the Project: Cellular SiC ceramics from Plant Precursor for engineering applications, Department of Science and Technology, Government of India, No. SR/S3/ME/20/2003-SERC-ENGG, September, 2008.

[28] O.P. Chakrabarti, J. Mukerji, Oxidation kinetics of reaction sintered silicon carbide, Bull. Mater. Sci. 16 (4) (1993) 325–329.